Int. J. Heat Mass Transfer. Vol. 31, No. 10, pp. 2005–2012, 1988
Printed in Great Britain

0017–9310/88 $3.00 + 0.00

Heat transfer in tissues radiated by a 432 MHz directional antenna

D. A. KOUREMENOS and K. A. ANTONOPOULOS
Mechanical Engineering Department, National Technical University of Athens, 42 Patission Street, Athens 106 82, Greece

(*Received* 15 *July* 1987)

Abstract—Heat transfer in tissues during electromagnetic heating obtained by a 432 MHz directional antenna for therapeutic purposes is considered. The two-dimensional transient heat conduction equation, which takes into account the electromagnetic heating and the cooling owing to blood circulation is solved by finite-difference means. Solutions in cases of inhomogeneous tissues and of tissues containing large blood vessels are given. Also, the analytical solution of the corresponding one-dimensional steady-state problem in the principal axis of the electromagnetic field is derived. This solution is in good agreement with the two-dimensional numerical solution and may therefore be employed for making quick calculations.

1. INTRODUCTION

HEATING of malignant tissues for therapeutic purposes using electromagnetic fields has recently become increasingly interesting. The treatment, known as hyperthermia, involves heating of tumour tissue in the temperature range 42–46°C for a specified period of time, usually 30–60 min. Temperature values within this range are not directly harmful to normal cells while it is hoped that cancerous ones are destroyed as they are more sensitive to high temperatures. Hyperthermia may be 'whole body', 'regional' or 'localized'. In the last case, which is of interest here, the heating of the tissue may be due to absorbed electromagnetic radiation transmitted by emitting antennas, placed on the surface of the skin, as shown in Fig. 1. Related surveys on the subject may be found in refs. [1, 2].

One of the most important points on tissue heat transfer is the blood vessels, which actually form the basic difference between tissue and solid media. According to the conventional bioheat transfer theory [3], valid for nearly 40 years, the effect of blood vessels is taken into account by including in the heat transfer differential equation a sink term, which is the product of the blood mass flow rate, of the blood specific heat and of the difference between the local and the body core temperature [3]. Latest heat transfer models [4–7], suggest that the above sink term does not succeed in describing heat transfer processes in vascularized tissues. Instead, they propose that the small vessels, which are always at local tissue temperature, may be taken into account collectively by introducing a slightly enhanced effective thermal conductivity [4]. The large discrete vessels should be described separately [6, 7], i.e. as heat sink lines of the actual body core temperature. Lastly, the treatment for the vessels of intermediate size depends on many parameters and falls between the collective description and the individual description. However, in many instances medium size vessels may be described collectively by using a greatly enhanced effective thermal conductivity.

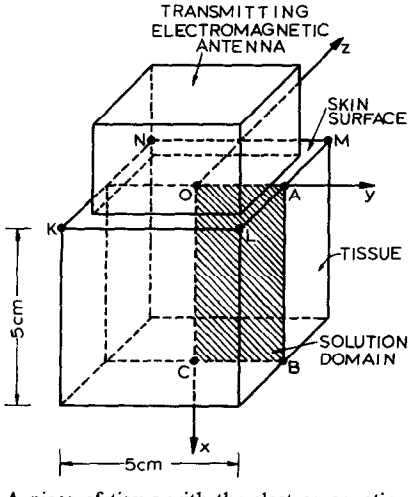

FIG. 1. A piece of tissue with the electromagnetic antenna and the solution domain OABC.

The numerical algorithm employed in the present study is based on conventional finite-difference techniques and solves the two-dimensional transient problem [8, 9]. The algorithm may be used either with the conventional blood heat sink term or with the new enhanced effective thermal conductivity model in conjunction with the individual description of large blood vessels. Variable properties of the tissue may be taken into account and any type of local hyperthermia system may be dealt with provided that the pattern of the antenna and therefore the function describing the distribution of the specific energy absorption rate within the tissue is known.

Application of the above algorithm is made in the

NOMENCLATURE

a, b, c, s	antenna constants measured in m^{-1}, m^{-1}, m, kg^{-1}, respectively	Q_R	heat source owing to absorbed electromagnetic radiation [$W m^{-3}$]
a_n	coefficient in finite-difference equation	S_U, S_P	source terms in finite-difference equation
C	tissue specific heat [$J kg^{-1} K^{-1}$]	t	time [s]
C_b	blood specific heat [$J kg^{-1} K^{-1}$]	T	local tissue temperature [°C]
G	a large number, e.g. 10^{30}	T_b	blood temperature, 37°C
k	tissue thermal conductivity [$W m^{-1} K^{-1}$]	T_s	temperature of the skin surface
P	antenna power [W]	W_b	blood mass flow rate per unit volume of tissue [$kg m^{-3} s^{-1}$]
Q_b	heat sink owing to blood circulation [$W m^{-3}$]	x, y, z	Cartesian coordinates [m].
Q_m	heat source owing to metabolic process [$W m^{-3}$]	Greek symbol	
		ρ	tissue density [$kg m^{-3}$].

case of the 432 MHz directional antenna developed by ref. [10]. Figure 2, discussed later, shows the distribution of the dimensionless energy generated within the tissue, corresponding to this antenna. The results include temperature contours at various time steps and a parametric study in the steady state. Solutions in cases of inhomogeneous tissues and of tissues containing large blood vessels are given. Also, the analytical solution of the one-dimensional steady-state problem is derived along the symmetry axis of the antenna. Good agreement is observed between the analytical solution and the two-dimensional numerical solution, thus suggesting that the former may be employed for making quick calculations with good accuracy.

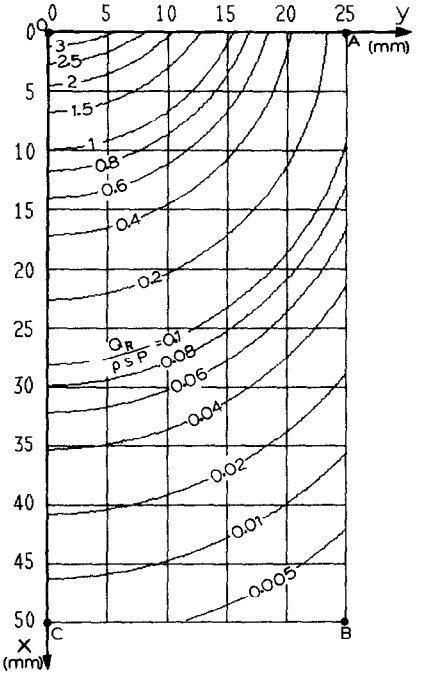

FIG. 2. Lines of constant dimensionless heat generation $Q_R/\rho sP$ within the solution domain OABC, according to equation (2) for antenna constants $a = -127\ m^{-1}$, $b = -129\ m^{-1}$, $c = 0.0245$ m.

2. DIFFERENTIAL EQUATION AND BOUNDARY CONDITIONS

With reference to Fig. 1, the two-dimensional heat conduction equation may be written as

$$\rho C\frac{\partial T}{\partial t} = \frac{\partial}{\partial x}\left(k\frac{\partial T}{\partial x}\right)+\frac{\partial}{\partial y}\left(k\frac{\partial T}{\partial y}\right)+Q_R+Q_m-Q_b \quad (1)$$

where T is the local temperature, x, y denote the Cartesian coordinates, t the time and ρ, C and k the density, the specific heat and the thermal conductivity of the tissue, respectively. The term Q_R represents the heat generated per unit volume of tissue, owing to the electromagnetic radiation absorbed. In general, it may be any function of the space and time coordinates and in the present case it is of the form [10]

$$Q_R = \rho sP e^{a(x-0.01)} e^{by^2/(x+c)} \quad (2)$$

where s, a, b, c are the antenna constants and P the transmitted power, which may be varied depending on the application requirements.

The term Q_b represents a heat sink, owing to blood circulation, which according to the conventional bioheat transfer theory may be expressed as [3]

$$Q_b = W_b C_b (T - T_b) \quad (3)$$

where T_b stands for the blood temperature which may be taken either constant or variable as the blood is heated passing through the tissue, W_b denotes the mass flow rate of the blood per unit volume of tissue and C_b is the blood specific heat. The large blood vessels are taken into account individually by considering internal cooling passages of fixed temperature (37°C).

Lastly, the term Q_m in equation (1) represents the heat generated by the metabolic process and is taken

approximately equal to zero, as it is very small compared to the term Q_R.

It can be seen from equation (2) and Fig. 2 that near the skin surface ($x \simeq 0$) high values of heat Q_R are generated thus causing dangerously high temperatures to appear there. Therefore, cooling of the skin surface at $T_s < 37°C$ should be attempted in order to decrease the high values of temperature and force the high-temperature region deeper into the tumour.

With reference to Fig. 1, the boundary conditions are as follows: on boundary OC of element OCBA, which is an axis of symmetry, the heat flux is equal to zero. On boundaries AB and BC, which are considered to be removed enough, a temperature of 37°C is prescribed. Lastly, the surface of the skin OA is cooled at a prescribed temperature T_s.

3. NUMERICAL SOLUTION OF THE TWO-DIMENSIONAL TRANSIENT PROBLEM

Solution of differential equation (1) is performed within the solution domain OABC of Fig. 1, by a standard finite-difference technique. Briefly, a Cartesian grid composed of coordinate lines is imposed on the solution domain, and differential equation (1) is cast into finite-difference form by integration over the control volumes of the grid and by averaging over a finite increment of time using an implicit scheme [11]. The resulting finite-difference equation for each node P of the grid is of the form

$$\left(\sum_n a_n - S_P\right) T_P = \sum_n a_n T_n + S_U, \quad n = N, S, E, W \tag{4}$$

where the summation is over the four neighbours N, S, E, W of the typical node P and the expression for the coefficients a and S may be found in ref. [11] among others. One equation of the form of equation (4) is written for each node P of the computational grid, thus resulting in a set of simultaneous algebraic equations, which is solved by using known iterative techniques [11].

In the case of a large blood vessel contained within the solution domain, it is desired that the temperature at the location of the vessel be held at a specified temperature T_b. This is obtained by specifying at the location of the vessel

$$S_U = GT_b \tag{5}$$

$$S_P = -G \tag{6}$$

where G is a large number (e.g. 10^{30}). It is easy to see that because of relations (5) and (6), equation (4) will give $T = T_b$ at the desired grid nodes.

4. ANALYTICAL SOLUTION OF THE ONE-DIMENSIONAL STEADY-STATE PROBLEM

In the one-dimensional steady-state case in the x-direction (Fig. 1), differential equation (1) with Q_R and Q_b taken from equations (2) and (3), respectively, the Q_m being zero, is reduced to

$$k\frac{d^2T}{dx^2} + \rho s P e^{a(x-0.01)} - W_b C_b (T - T_b) = 0. \tag{7}$$

The above equation may be integrated in the region $x = 0$–l with boundary conditions

$$T = T_s \quad \text{at } x = 0 \tag{8}$$

$$T = 37°C \quad \text{at } x = l \tag{9}$$

to yield

$$\frac{T-37}{T_s-37} = \frac{\sinh(m(l-x))}{\sinh(ml)} - \frac{F}{T_s-37}\left[\frac{\sinh(m(l-x))}{\sinh(ml)} + e^{al}\frac{\sinh(mx)}{\sinh(ml)} - e^{ax}\right] \tag{10}$$

where

$$m = (W_b C_b/k)^{1/2} \tag{11}$$

$$F = \frac{\rho s P e^{-a/100}}{k(m^2 - a^2)}. \tag{12}$$

5. RESULTS

In the calculations presented here, the antenna constants have been fixed to the typical values $s = 12.5\ \text{kg}^{-1}$, $a = -127\ \text{m}^{-1}$, $b = -129\ \text{m}^{-1}$, $c = 0.0245$ m. Figure 2 shows lines of constant energy, generated within the solution domain, in the dimensionless form $Q_R/\rho sP$, calculated according to equation (2) with the above values of the antenna constants.

5.1. *Variation of the temperature field with time*

An example of the results of the numerical solution is given in Figs. 3(a)–(c) which show isotherms at times $t = 1$, 4 and 10 min (steady state), respectively, with the initial temperature field taken 37°C everywhere. These results correspond to the following values of the parameters involved: $\rho = 1000\ \text{kg m}^{-3}$, $C = 4180\ \text{J kg}^{-1}\ \text{K}^{-1}$, $k = 0.5016\ \text{W m}^{-1}\ \text{K}^{-1}$, $P = 20$ W, $W_b = 8\ \text{kg m}^{-3}\ \text{s}^{-1}$, $C_b = 3344\ \text{J kg}^{-1}\ \text{K}^{-1}$, $T_s = 20°C$. The maximum temperature $T_{max} = 43.3°C$ is observed in Fig. 3(c) on the axis of symmetry $y = 0$ at a depth of 9 mm from the surface of the skin.

In the above example, as in almost all cases examined, the fully steady state is reached, with accuracy 0.1°C, at $t = 10$ min, although the temperature field is very close to the steady state considerably earlier. Thus, at $t = 6$ and 8 min the temperature field has reached 99 and 99.5% of the steady-state solution. The greater delay to reach the steady state is observed on the axis of symmetry $y = 0$ in the region of high temperatures, as expected.

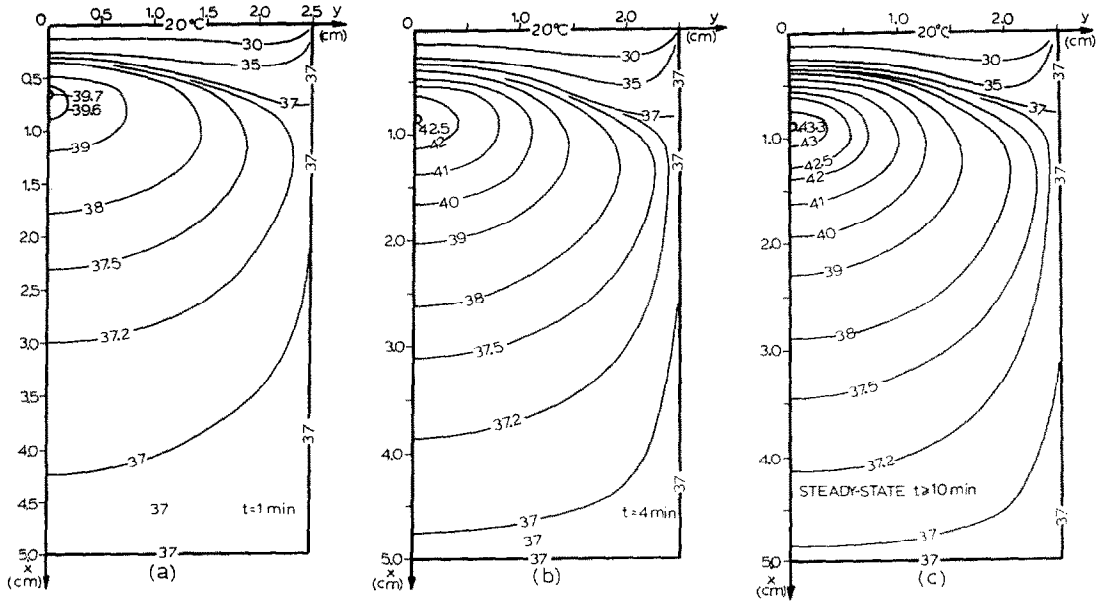

FIG. 3. Predicted isotherms at times $t = 1$, 4 and $t \geqslant 10$ min (steady state) for $\rho = 1000$ kg m^{-3}, $C = 4180$ J kg^{-1} K^{-1}, $k = 0.5016$ W m^{-1} K^{-1}, $P = 20$ W, $W_b = 8$ kg m^{-3} s^{-1}, $C_b = 3344$ J kg^{-1} K^{-1}, $T_s = 20$°C.

5.2. *Parametric study in the steady state*

Because of the numerous parameters involved in the governing differential equation (1), a generalization of the results is very difficult.

For a specified kind of antenna (i.e. for fixed values of the antenna constants) the main parameters influencing the problem are: the transmitted power P, the mass flow rate of the blood per unit volume of tissues W_b, the temperature T_s at which the surface of the skin is cooled, and the thermal conductivity k of the tissue. Numerical solutions of differential equation (1) have been obtained for values of the above parameters in the following ranges:

$$P = 15\text{–}30\,\text{W}$$

$$W_b = 5\text{–}9\,\text{kg m}^{-3}\,\text{s}^{-1}$$

$$T_s = 10\text{–}30^\circ\text{C}$$

$$k = 0.4\text{–}0.8\,\text{W m}^{-1}\,\text{K}^{-1}$$

with the remaining parameters fixed at the usual values $\rho = 1000$ kg m^{-3}, $C = 4180$ J kg^{-1} K^{-1}, $C_b = 3344$ J kg^{-1} K^{-1}. Figure 4 shows the temperature variation along the axis of symmetry OC in 16 cases defined by the limits of the above ranges. In the same figure, the one-dimensional analytical solution according to equation (10) is also presented, which is in good agreement with the numerical two-dimensional solution.

With reference to the above mentioned figure, it is seen that the effect of all main parameters P, W_b, T_s and k is considerable. As expected, temperatures increase with increasing transmitted power P and decrease with increasing blood mass flow rate W_b. The effect of lowering surface temperature T_s is to decrease the maximum temperature developed and to force its location deeper into the tissue. Lastly, high values of the tissue thermal conductivity result in more uniform temperature variations and lower maximum temperatures.

In the range of parameters examined, the lowest temperatures are developed in the case of $P = 15$ W, $W_b = 9\,\text{kg m}^{-3}\,\text{s}^{-1}$, $T_s = 10^\circ\text{C}$ and $k = 0.8\,\text{W m}^{-1}\,\text{K}^{-1}$, i.e. a maximum temperature $T_{max} \simeq 39^\circ$C is obtained, which is not high enough for therapeutic purposes. Therefore, in this case of high values of the tissue properties W_b and k, higher values of P and T_s have to be employed. At the other end of the range, for $P = 30$ W, $W_b = 5$ kg m^{-3} s^{-1}, $T_s = 30^\circ$C and $k = 0.4$ W m^{-1} K^{-1}, the highest temperatures are observed with $T_{max} \simeq 57^\circ$C, which is harmful and therefore lower values of P and T_s must be employed.

In conclusion, the above discussed Fig. 4 which shows the curves for the limiting values of the tissue properties (k, W_b) and of the conditions of application (P, T_s), can be used in practice as a guide showing the maximum temperature expected. Further, because of the close agreement of the one-dimensional analytical solution, given by equation (10), with the two-dimensional numerical solution, the former may be employed for calculating accurately enough and very quickly the expected temperature variation along the antenna axis for any values of the parameters involved and of the antenna constants. The derived analytical solution may be particularly useful for on-line calculations with microcomputers connected with hyperthermia systems, a task towards which recent efforts are directed.

5.3. *Variable tissue properties*

In reality, the properties of the tumour are different to those of the normal tissue. Therefore, it is of interest

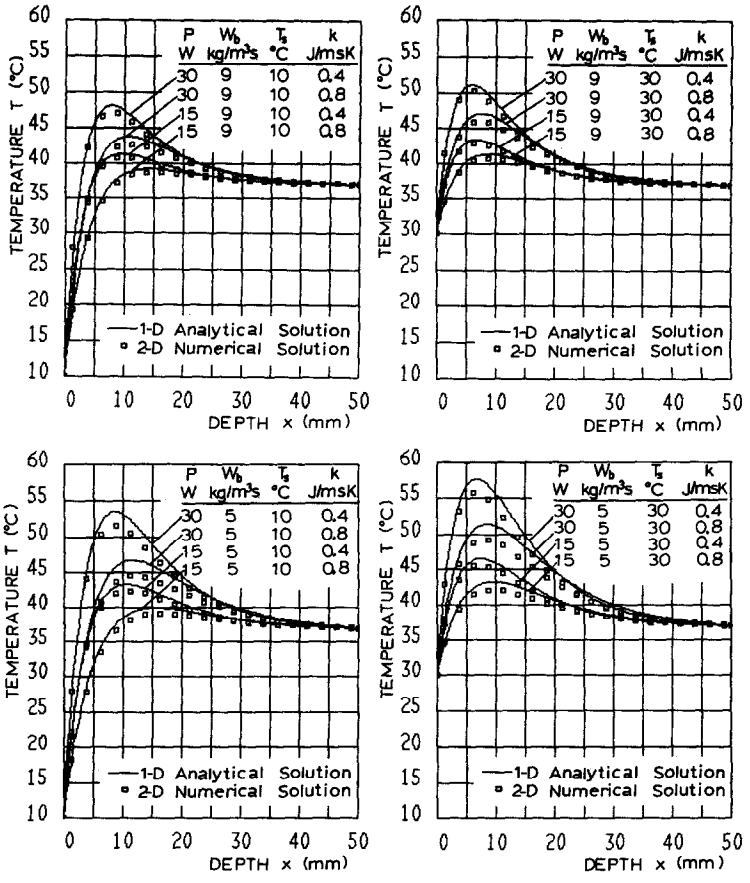

FIG. 4. Calculated temperature variation in the steady state along the axis of symmetry OC for various values of the main parameters P, W_b, T_s, k with the remaining parameters fixed at the usual values $\rho = 1000\ \text{kg m}^{-3}$, $C = 4180\ \text{J kg}^{-1}\ \text{K}^{-1}$, $C_b = 3344\ \text{J kg}^{-1}\ \text{K}^{-1}$.

to examine such cases. An example is given in Fig. 5. The shaded area represents a likely location of the tumour. Inside this area the thermal conductivity and the blood mass flow rate have been taken as $k_{in} = 0.4\ \text{W m}^{-1}\ \text{K}^{-1}$ and $(W_b)_{in} = 5\ \text{kg m}^{-3}\ \text{s}^{-1}$, respectively. Outside the tumour area they have been fixed to the usual values $k_{out} = 0.5016\ \text{W m}^{-1}\ \text{K}^{-1}$, $(W_b)_{out} = 8\ \text{kg m}^{-3}\ \text{s}^{-1}$. The remaining properties, which seem to be rather insensitive to tissue changes, are considered constant throughout the field, i.e. $\rho = 1000\ \text{kg m}^{-3}$, $C = 4180\ \text{J kg}^{-1}\ \text{K}^{-1}$, $C_b = 3344\ \text{J kg}^{-1}\ \text{K}^{-1}$, and the application parameters, in this example, are taken as $P = 20$ W, $T_s = 20°\text{C}$.

Comparison of the steady-state isotherms of Fig. 5 to those of Fig. 3(c) shows the effect of the decreased blood mass flow rate and thermal conductivity within the tumour area. As expected higher temperatures are developed in the case of Fig. 5, especially within the tumour (maximum temperature 46.2°C as compared to 43.3°C) owing to the reduced conductivity and cooling.

Figure 6 shows a parametric study in the case of a tumour lying at the same location and under the same conditions as above. Here, variables are the thermal conductivity and the blood mass flow rate inside the tumour, which are varied in the range $k_{in} = 0.4$–$0.8\ \text{W m}^{-1}\ \text{K}^{-1}$, $(W_b)_{in} = 5$–$9\ \text{kg m}^{-3}\ \text{s}^{-1}$. The figure shows the variation of the maximum temperature T_{max} of the field as a function of $(W_b)_{in}$ with k_{in} as a parameter. It is seen that, in the ranges of k_{in} and $(W_b)_{in}$ examined, the influence of k_{in} is strong at the low values of $(W_b)_{in}$ and causes a 3°C change of T_{max}, while at the high values of $(W_b)_{in}$ it is weak and causes a change of about 1.5°C. Similarly, the influence of $(W_b)_{in}$ is strong at the low values of k_{in} and weak at the high values.

5.4. *Effect of large vessels*

As mentioned in the Introduction, the large vessels (arteries or veins) cannot be described collectively, i.e. by the heat sink term Q_b (equation (3)) or by introducing an enhanced effective thermal conductivity [4], but they have to be taken into account individually. Solutions for various geometries with discrete large vessels have been obtained in conjunction with the directional antenna under consideration (equation (2)). Examples of calculated temperature contours are shown in Figs. 7(a)–(c), in which the influence of small vessels on tissue heat transfer has been taken into account by the usual sink Q_b method and the following values have been given to the parameters involved:

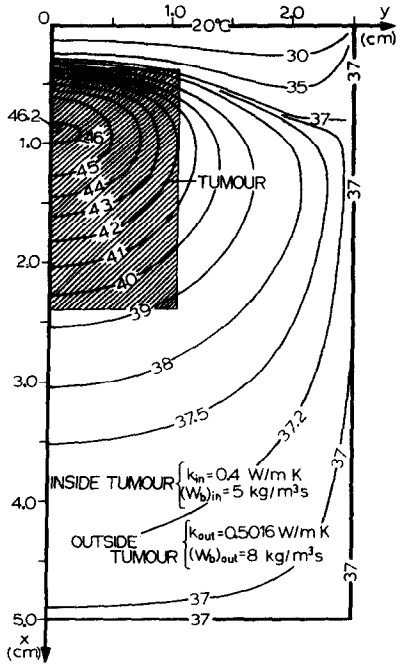

FIG. 5. Predicted steady-state isotherms in the case when the thermal conductivity and the blood mass flow rate within the tumour (shown shaded) are $k_{in} = 0.4$ W m^{-1} K^{-1} and $(W_b)_{in} = 5$ kg m^{-3} s^{-1}, respectively, while outside the tumour they are $k_{out} = 0.5016$ W m^{-1} K^{-1}, $(W_b)_{out} = 8$ kg m^{-3} s^{-1}. The remaining parameters have the values $\rho = 1000$ kg m^{-3}, $C = 4180$ J kg^{-1} K^{-1}, $C_b = 3344$ J kg^{-1} K^{-1}, $P = 20$ W, $T_s = 20$°C.

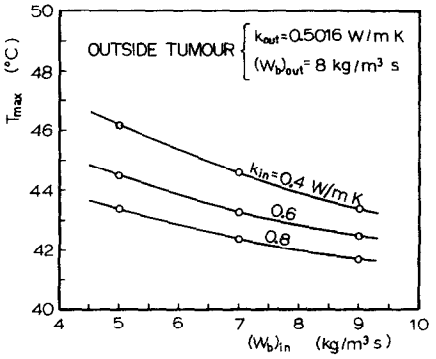

FIG. 6. Predicted maximum temperature in the steady state as a function of the blood mass flow rate $(W_b)_{in}$ inside the tumour for various values of the thermal conductivity k_{in} inside the tumour. The values of the above properties outside the tumour are $(W_b)_{out} = 8$ kg m^{-3} s^{-1}, $k_{out} = 0.5016$ W m^{-1} K^{-1}. The values of the remaining parameters and the location of the tumour are the same as in Fig. 5.

$\rho = 1000$ kg m^{-3}, $C = 4180$ J kg^{-1} K^{-1}, $k = 0.5016$ W m^{-1} K^{-1}, $P = 20$ W, $W_b = 8$ kg m^{-3} s^{-1}, $C_b = 3344$ J kg^{-1} K^{-1}, $T_s = 20$°C.

Comparison of Figs. 3(c) and 7(a) shows that when a vessel is located away from the axis of symmetry of the antenna ($y = 0$), its effect will be a local change in the temperature field without affecting the location and the level of the maximum temperature. However, when the vessel lies on $y = 0$, as shown in Figs. 7(b) and (c), the closer it is to the location of the maximum temperature the more important its effect will be. Thus, for $x = 6$ mm (Fig. 7(b)) the vessel causes the maximum temperature to drop from 43.3 to 42°C and to move the maximum temperature location deeper and away from the axis of symmetry, while for $x = 9$ mm (Fig. 7(c)) these effects are stronger.

6. CONCLUSION

A finite-difference solution has been given for the two-dimensional transient heat transfer problem in tissues during local hyperthermia with a 432 MHz directional antenna. The method of solution is general and may be used with various types of hyperthermia systems and either with the conventional blood heat sink term or by the new enhanced effective thermal conductivity models in conjunction with an individual description of the large blood vessels. Also, the analytical solution of the corresponding one-dimensional steady-state problem has been derived.

The main conclusions are summarized below.

(a) The fully steady state is reached with accuracy 0.1°C at $t = 10$ min, although the temperature field is very close to the steady state considerably earlier. Thus, at $t = 6$ and 8 min the temperature field has reached 99 and 99.5%, respectively, of the steady-state solution.

(b) Since a generalization of the results was difficult, owing to the numerous parameters involved, solutions corresponding to limiting values of the main parameters have been given. These solutions may be used in practice as a guide showing the expected temperatures developed. In the ranges examined, the maximum temperature of the field, which is obtained on the axis of symmetry, varies from about 39°C (for $P = 15$ W, $W_b = 9$ kg m^{-3} s^{-1}, $T_s = 10$°C, $k = 0.8$ W m^{-1} K^{-1}) to about 57°C (for $P = 30$ W, $W_b = 5$ kg m^{-3} s^{-1}, $T_s = 30$°C, $k = 0.4$ W m^{-1} K^{-1}). The depth, measured from the skin surface, where the maximum temperature is located, varies from 6 to 16 mm corresponding to cooling of the skin surface at 30 and 10°C.

(c) The analytical solution of the corresponding one-dimensional problem in the principal axis of the electromagnetic field is in good agreement with the numerical two-dimensional solution. Therefore, the former may be employed for making quick calculations with good accuracy. The derived analytical solution may be particularly useful for microcomputer on-line calculations connected with hyperthermia systems, a task towards which recent efforts have been directed.

(d) The effect of different thermal conductivity and blood mass flow rate within the normal and the neoplastic tissue has been examined. Changes of the maximum temperature of up to 5°C have been

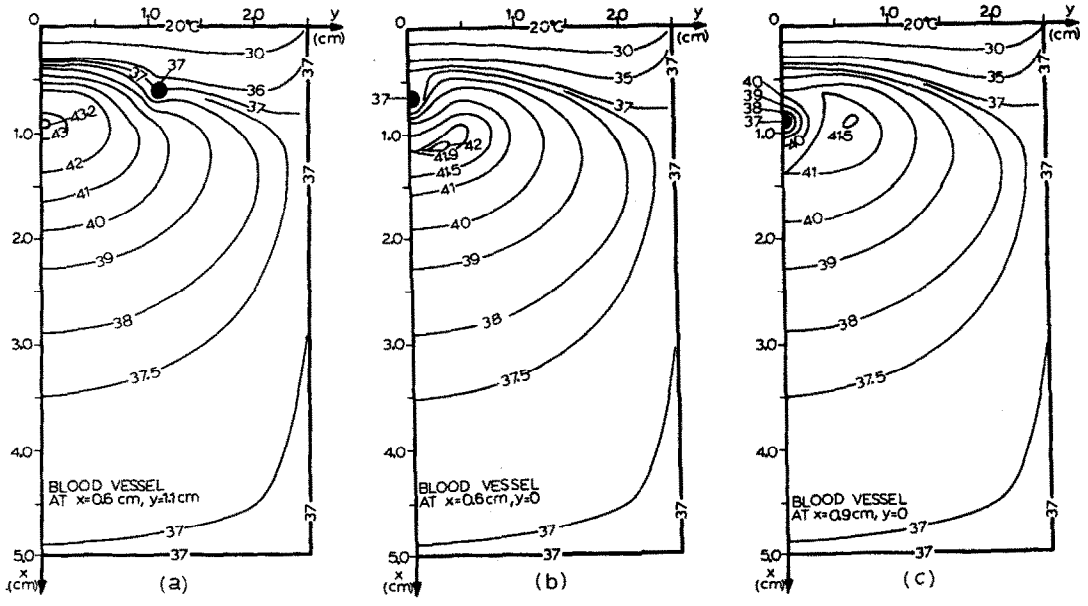

FIG. 7. Predicted steady-state isotherms in the case of tissue containing a large blood vessel located at: (a) $x = 0.6$ cm, $y = 1.1$ cm; (b) $x = 0.6$ cm, $y = 0$; (c) $x = 0.9$ cm, $y = 0$. The values of the parameters involved are the same as in Fig. 3.

observed in respect of the tumour dimensions considered and the ranges of variables under examination.

(e) Solutions obtained in the case of tissues containing large blood vessels showed that when a large vessel is located away from the principal axis of the electromagnetic field, its effect will be only a local change in the temperature field. When the vessel lies on the principal axis, it causes a considerable drop of the maximum temperature and a considerable displacement of its location away from the axis.

REFERENCES

1. J. W. Strohbehn and R. B. Roemer, A survey of computer simulations of hyperthermia treatments, *IEEE Trans. Biomed. Engng* **BME-31**(1), 136–149 (1984).
2. R. J. Spiegel, A review of numerical models for predicting the energy deposition and resultant thermal response of humans exposed to electromagnetic fields, *IEEE Trans. Microwave Theory Techniques* **MTT-32**(8), 730–746 (1984).
3. H. H. Pennes, Analysis of tissue and arterial blood temperatures in the resulting human forearm, *J. Appl. Physiol.* **1**, 93–122 (1948).
4. M. M. Chen and K. R. Holmes, Micro-vascular contributions in tissue heat transfer, *Ann. N.Y. Acad. Sci.* **35**, 137–151 (1980).
5. J. J. W. Lagendijk, The influence of blood flow in large vessels on the temperature distribution in hyperthermia, *Phys. Med. Biol.* **27**, 17–23 (1982).
6. J. J. W. Lagendijk, M. Schellekens, J. Schipper and P. M. van der Linden, A three-dimensional description of heating patterns in vascularized tissues during hyperthermia treatment, *Phys. Med. Biol.* **29**, 495–507 (1984).
7. J. Mooibroek and J. J. W. Lagendijk, Design of a three-dimensional thermal model for inhomogeneous and vascularized tissues, *Strahlentherapie* **161**, 545–546 (1985).
8. D. A. Kouremenos and K. A. Antonopoulos, Numerical simulation of the thermal problem in hyperthermia treatments, *Proc. Fifth Int. Conf. on Numerical Methods in Thermal Problems*, Montreal, Part 1, pp. 276–283 (1987).
9. D. A. Kouremenos and K. A. Antonopoulos, Finite-difference solution of the transient bioheat transfer equation during local hyperthermia in inhomogeneous tissues containing arteries and veins, *Proc. Fifth Int. Conf. on Numerical Methods in Thermal Problems*, Montreal, Part 1, pp. 811–820 (1987).
10. N. K. Uzunoglu, E. A. Angelikas and P. A. Cosmidis, A 432-MHz local hyperthermia system using an indirectly cooled, water-loaded waveguide applicator, *IEEE Trans. Microwave Theory Techniques* **MTT-35**, 106–111 (1987).
11. G. D. Smith, *Numerical Solution of Partial Differential Equations*. Oxford University Press, Oxford (1974).

TRANSFERT THERMIQUE DANS DES TISSUS CAUSE PAR UNE ANTENNE DIRECTIONNELLE A 432 MHz

Résumé—On considère le transfert thermique dans des tissus pendant le chauffage électromagnétique obtenu avec une antenne directionnelle à 432 MHz pour des buts thérapeutiques. L'équation du transfert de chaleur bidimensionnel tenant compte du chauffage électromagnétique et du refroidissement par la circulation sanguine est résolue par la méthode des différences finies. On donne des solutions pour des tissus non homogènes et des tissus contenant de gros vaisseauz sanguins. On dérive aussi la solution analytique du problème permanent et monodimensionnel dans l'axe principal du champ électromagnétique. Cette solution est en bon accord avec la solution numérique bidimensionnelle et elle peut être employée dans des calculs rapides.

WÄRMETRANSPORT IN ZELLGEWEBEN INFOLGE EINER GERICHTETEN ELEKTROMAGNETISCHEN MHZ-BESTRAHLUNG

Zusammenfassung—Es wird der Wärmetransport in Zellgewebe beim elektromagnetischen Heizen mit Hilfe einer 432 MHz-Richtantenne für therapeutische Anwendungen untersucht. Die zweidimensionale instationäre Wärmeleitgleichung wird unter Berücksichtigung des elektromagnetischen Heizens und der durch Blutzirkulation verursachten Kühlung mit Hilfe eines Finite-Differenzen-Verfahrens gelöst. Es werden Lösungen angegeben für den Fall inhomogener Zellgewebe und für Zellgewebe mit großen Blutgefäßen. Desweiteren wird die analytische Lösung des entsprechenden eindimensionalen stationären Falls in der Hauptachse des elektromagnetischen Feldes hergeleitet. Diese Lösung stimmt mit der zweidimensionalen numerischen Lösung gut überein und kann daher für überschlägige schnelle Berechnungen verwendet werden.

ТЕПЛОПЕРЕНОС В ТКАНЯХ ПОД ВОЗДЕЙСТВИЕМ ИЗЛУЧЕНИЯ С ЧАСТОТОЙ 432 МГц ОТ НАПРАВЛЕННОЙ АНТЕННЫ

Аннотация—Рассматривается теплоперенос в тканях при нагреве электромагнитным излучением с частотой 432 МГц от направленной антенны, используемого в терапевтических целях. Методом конечных разностей решено двумерное нестационарное уравнение теплопроводности с учетом электромагнитного нагрева тканей и их охлаждения за счет циркуляции крови. Решения даны для неоднородных тканей и для тканей с крупными кровеносными сосудами. Получено также аналитическое решение соответствующей одномерной стационарной задачи по главной оси электромагнитного поля. Аналитическое решение хорошо согласуется с двумерным численным решением и поэтому может использоваться для быстрых расчетов.